www.ijecs.in
International Journal Of Engineering And Computer Science ISSN:2319-7242
Volume 2 Issue 5 May, 2013 Page No. 1457-1464

A REVIEW ON RIPPLE CURRENT REDUCTION TECHNIQUE WITH ACTIVE POWER FILTER

Tembhurnikar Gaurav[1], Gajare Pankaj[2], Wani Nilesh[3], Patil Nitin[4]
[1,2,3,2]*Shri Sant Gadge Baba College of Engineering and Technology Bhusawal, India*
tgaurav81@gmail.com
pnkjgjre@gmail.com
nileshswani@gmail.com
patil.nitinr@gmail.com

Abstract —This paper presents the estimation of ripples by using analytical method in active power filters .This method is based on an average model of PWM voltage source inverter. The formulae for the ripple magnitude are derived for single-phase and three-phase three-leg structures. Numerical examples for filters generating third and fifth order harmonics are presented. The reactive component of fundamental harmonic is considered as an example. A ripple current reduction method is proposed that does not require additional switching devices. A current ripple having twice the frequency component of the power supply is generated in the dc part when a single-phase pulse width-modulated inverter is used for a grid connection. The current ripple causes shortening of the lifetime of electrolytic capacitors, batteries, and fuel cells. Without increasing the number of switching devices, the proposed circuit realizes a dc active filter function because center tap of the isolation transformer is connected to the energy buffer capacitor.In addition, the buffer capacitor voltage is controlled by the common-mode voltage of the inverter. The features of the proposed circuit, control strategy, and experimental results are described, including the result of ripple reduction, to approximately 20% that of the conventional circuit.

Key words: low frequency ripple, fuel cell systems, ripple current reduction, single phase isolated converter

I. INTRODUCTION

In response to global warming and environmental issues, energy sources such as wind power systems, photovoltaic cells, and fuel cells have been extensively studied recently. The fuel cell is an important technology for new mobile applications and power grid distribution systems. For power distribution, in order to supply power to the power grid, a fuel cell system requires a grid interconnection converter. This converter using an isolation transformer is preferable for power grid distribution systems such that it provides protection against surges and reduces noise. In addition, essential requirements are size reduction and high efficiency [1]-[8]. One of the problems in this system is that the ripple current decreases the lifetime and hence, the fuel cell ripple current must be reduced in the grid interconnection converter[9]-[10]. However, when a single-phase pulse width-modulated (PWM) inverter is used for grid connection system, the power ripple is twice the frequency of the power grid. Therefore, large electrolytic capacitors are connected in parallel to the fuel cell to reduce the current ripple in conventional grid connection inverters. However, the ripple effect is an important feature of power electronic circuits working in switching scheme. Switching frequency errors are undesirable effects with these techniques. Additional filters are used to eliminate the Ripple errors. Properly chosen switching algorithms can minimize the ripple effects The current ripple's magnitude can be computed by simulation of a specific PWM realization. Analytical formulae will give more general information. Such formulae can be derived when an average model of PWM inverter is employed. The averaging approximates the discontinuous system by a time-continuous model. Average models simplify analysis, make the system's behavior easy to understand, speed up simulation and can be used for control and design purposes. The averaging method has been developed, for a wide class of power electronics circuits. The application of averaging techniques for STATCOM (Static Compensator) and active filters has been proposed as well in [11]. The use of large-sized electrolytic capacitors results in increased device volume as well as cost. Moreover, some approaches use high-speed current control

in order to reduce the current ripple in the fuel cell [12]-[13]. Here, a current-loop control is included within the existing dc–dc converter voltage loop. However, a large capacitor or reactor is required as an energy buffer. Other approaches have been proposed that do not require the use of large-sized electrolytic capacitors, e.g., an active filter is applied in the dc-link part[14]-[17]. The dc active filter has the following parts namely a small capacitor as an energy buffer, a reactor to reduce the switching ripple, and a dc chopper. The dc chopper injects the ripple current to avoid a power ripple. The capacitance can be lower, because the terminal voltage of the capacitor can be varied over a wide range but not without an increase in the number of the switching devices. This requires a high-cost dc chopper resulting in the undesirable large volume device. Similar problems exist with other configurations of dc active filters. This paper proposes a new circuit topology including a dc active filter function without extra switching devices. The proposed circuit consists of an isolated dc/dc converter and inter-connection inverter, and achieves the dc active filter function using the center tap of the isolation transformer. One feature of the proposed converter is that the common-mode volt-age and the differential voltage individually control the primary-side inverter in the dc/dc converter. The ripple current is suppressed by the common-mode voltage control of the dc/dc converter, and the main power flow is controlled by the differential-mode voltage. Conventional and proposed circuit topologies with the principle of current ripple suppression are first introduced. The control method of the proposed circuit is then described. In addition, the design of the energy buffer capacitor and transformer by which the maximum power ripple can be accepted is indicated. Furthermore, experimental results are presented in order to confirm the validity of the proposed circuit.

II. OVERVIEW OF ACTIVE POWER FILTERS

The general topology for the four wire active filter is shown in Fig. 1. A common capacitor is used by the dc bus, with the center-tap connected to the line neutral. The PWM pattern is generated using a constant frequency ramp comparison technique. The converter's ac side is connected to the mains via a synchronous link reactor L_{af} (Fig. 2), also serving as a first order low-pass filter. The current reference is the harmonic component of the load. Two options are available for harmonic extraction: i) use of a band-stop filter centered around the line frequency; ii) isolating the fundamental component by band-pass filter and then subtracting it from the load current. Option (ii) is chosen because phase shift and magnitude of the residual currents are lower in the practical implementation than for option (i). The error between the actual current and the reference current is processed through a PI controller in order to generate the gating signals, then the comparison of the output current error with a fixed amplitude and frequency triangular wave takes place as shown in Fig. 2. Thus, well defined spectral line frequencies occur for the switching frequency components of the output current of the converter. In order to cancel higher order load harmonics, a high current loop bandwidth is required. It is designed to have bandwidth as close as possible to the PWM modulator bandwidth, which is about half the switching frequency. The PI controller coefficients are selected according to [18]. DC bus voltage control is performed by adjusting the small amount of real power flowing into the dc capacitor, thus providing compensation for the converter and system losses. The design of the voltage loop is to be at least 10 times slower than the current loop; hence the two loops can be considered decoupled.

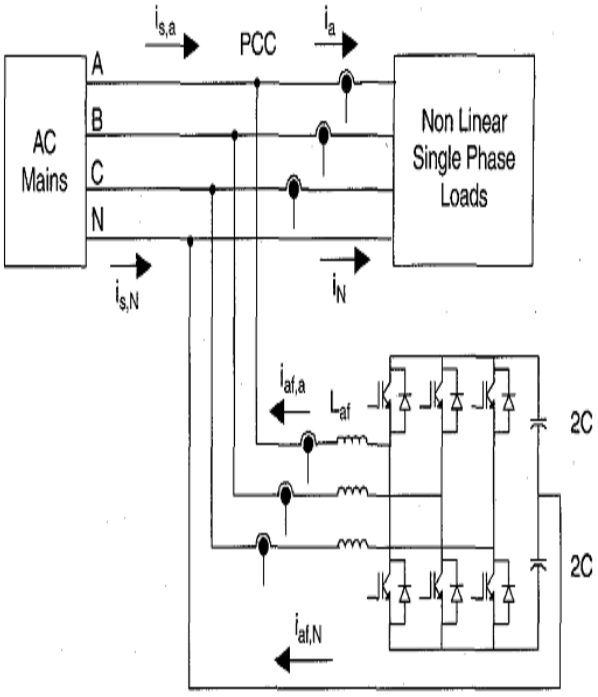

Fig. 1: Four wire half-bridge active filter.

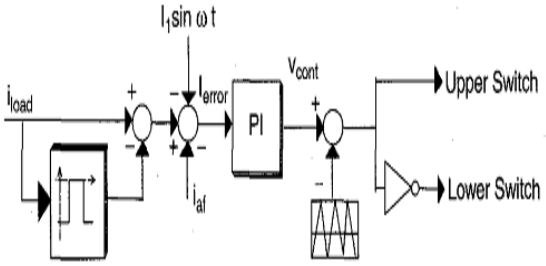

Fig. 2: Per phase current regulator.

III. SINGLE-PHASE VOLTAGE SOURCE INVERTER FOR RIPPLE ERROR DETECTION.

The deviation level of real generated current waveform from the smooth average waveform can be easily estimated for active power filters working with fixed switching frequency. The inverters working with fixed switching frequency inject harmonic components with frequency varying in narrow band. The single-phase topology of the voltage source inverter generating desired current waveform is shown in Fig. 3. A properly switched circuit should generate current as close to the reference signal as possible. The fixed switching frequency scheme with the switching periods T will be considered.

When the switching system operates in open loop, the switching transitions occur at predetermined times and time function s (t) takes the form of determined rectangular wave. Two modes will be considered – bipolar mode (Fig. 4a) and unipolar mode (Fig.4b).

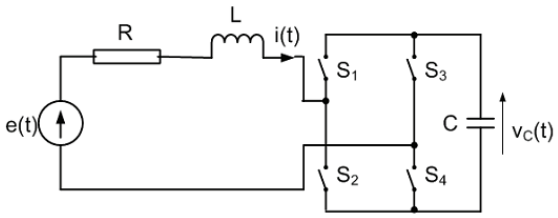

Fig. 3: Single-phase circuit generating current harmonics

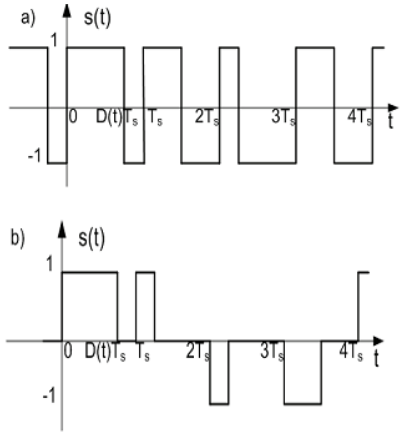

Fig. 4: Switching modes:- a) Bipolar b) Unipolar

IV. FUEL CELL EQUIVALENT CIRCUIT

The fuel cell stack internal impedance can be represented electrically by means of an equivalent circuit. The fuel cell exhibits complex internal impedance, which can be simplified by two R-C elements and a resistance connected in series (fig 5). In this equivalent circuit, the R-C elements represent the anode and cathode time constants and the resistance R_m is the membrane resistance. This circuit can be verified experimentally with the help of frequency spectrography and the Nyquist graph of the measured data. This can be observed in fig. 6 which clearly shows the two semi circles due to the R-C time constants and a distance to the reactance axis which shows the DC resistance of the stack. It is also observed from fig. 6 that the impedance of the fuel cell is load dependent but its shape is conserved for different load conditions, indicating that only the parameters of the equivalent circuit change with the load and not the equivalent circuit itself.

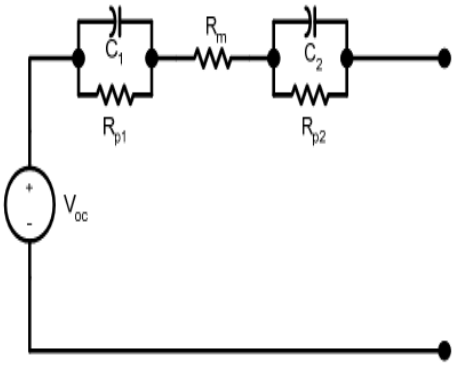

Fig. 5: Fuel cell equivalent circuit

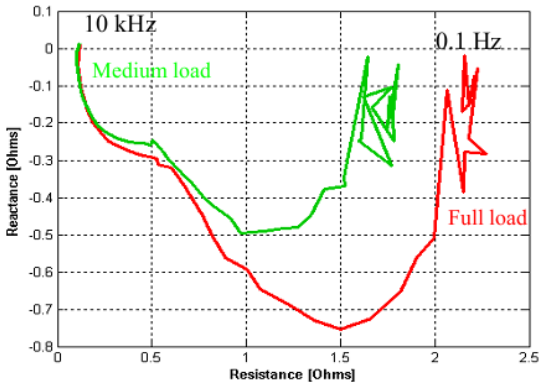

Fig. 6: Nyquist plot for a 30 W fuel cell stack

From the equivalent circuit shown in figure 5, it is possible to derive an expression for the impedance of the fuel cell stack in terms of the ripple frequency [19].

$$Z_{fc} = \left[\frac{R_1}{w^2 C_1^2 \left(R_1^2 + \frac{1}{w^2 C_1^2} \right)} + R_m + \frac{R_2}{w^2 C_2^2 \left(R_2^2 + \frac{1}{w^2 C_2^2} \right)} \right]$$

$$- I \left[\frac{R_1^2}{wC_1 \left(R_1^2 + \frac{1}{w^2 C_1^2} \right)} + \frac{R_2^2}{wC_2 \left(R_2^2 + \frac{1}{w^2 C_2^2} \right)} \right]$$

Accordingly the additional internal losses in the fuel cell produced by the ripple current can then be calculated using:

$$P_{loss,hf} = \Re(Z_{fc}(w_{ripple}))I^2_{ripple,rms}$$

Where w_{ripple} is the angular frequency of the ripple current and $I_{ripple,rms}$ is the rms value of the ripple current component. It can be seen from the above equation that as the frequency of the ripple current increases the real part of the fuel cell impedance is reduced to the membrane resistance Rm. Thus the additional internal losses produced by the ripple frequency also decrease as frequency increases. Fig. 7 shows the available power vs. frequency of ripple current obtained from the analysis. It can be observed from fig. 7 that if the current drawn from the stack has a low frequency ripple component (<1 kHz) the power that the fuel cell can deliver is reduced. On the other hand if the ripple current is of high frequency (1 kHz and above) the reduction in the available power is minimal.

As a result of this it can be seen that if the current drawn from the fuel cell contains ripple components of different frequencies, additional losses will be produced in the internal impedance of the stack. Due to these additional losses the power that the stack can supply to the load is reduced. Also, it is found that the available power at the stack terminals is a function of the frequency of the ripple current. It can be shown that due to this construction the current in the DC-link as well as the current drawn from the fuel cell contains a second harmonic current component.

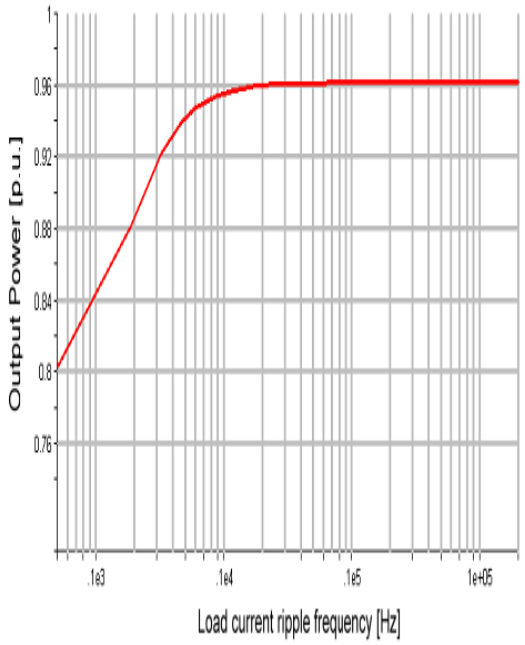

Figure 7: Fuel cell output power calculated from the equivalent circuit

However, low frequency harmonics in the current drawn from the stack leads to reduction of the power that the fuel cell can supply and increases stack heating. Thus to improve the system performance it is required to minimize or eliminate the low frequency current component. In addition, it can also be observed from the equivalent circuit that due to the R-C elements in the equivalent circuit its dynamics are relatively slow (about 30 ms for the dominant time constant), and that they do not have overload capability. So, an energy storage element such as batteries or super capacitor is required. This energy storage element is typically connected in parallel to the fuel cell or at the output terminals of the DC-DC converter. In which case, the connection is often times done through an additional DC-DC converter allowing the use of lower voltage storage elements.

V. INNOVATIVE CONVERTER

As shown in the previous paragraph, to improve fuel cell system performance in applications supplying power to single phase loads it is required to reduce or eliminate low frequency ripple in the current drawn from the fuel cell stack. It can be shown that the current in the DC-link between DC-DC converter and inverter is given by:

$$i_{DC-link} = I_d - \sqrt{2}I_{d2}\cos(2\omega t - \varphi)$$

Where I_d and I_{d2} in the above equation are calculated according to the equations given below, V_o is the output voltage of the inverter, Io its output current, V_d inverter DC-link voltage, and the phase angle of the load being supplied

$$I_d = \frac{V_o I_o}{V_d}\cos(\varphi)$$

$$I_{d2} = \frac{1}{\sqrt{2}}\frac{V_o I_o}{V_d}$$

The current given in the above equation is reflected to the input side of the DC-DC converter multiplied by its voltage gain. So, from the fuel cell point of view, the power conditioner can be modeled as a current sink drawing a current composed of DC, second harmonic and higher order terms corresponding to the switching frequencies of the DC-DC converter and inverter (fig. 8).

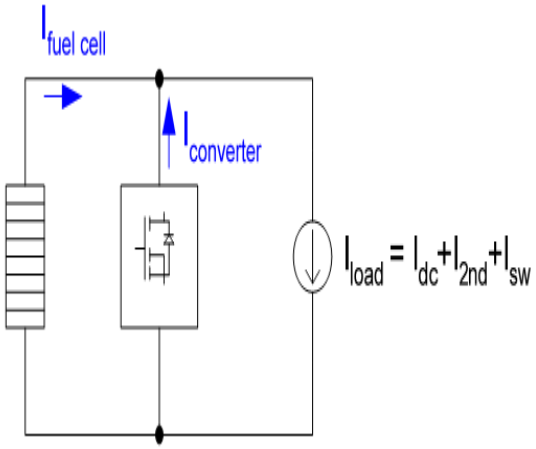

Fig. 8: System model

Using the above model, we observe that a feasible way to supply the low frequency current component drawn by the power conditioner is by a shunt power converter. This shunt converter can be operated in current mode and suitably controlled to supply the current required to improve fuel cell performance. Several topologies are available to implement the proposed shunt converter, however a back-boost DC-DC converter is selected on account of its simplicity and low part count.

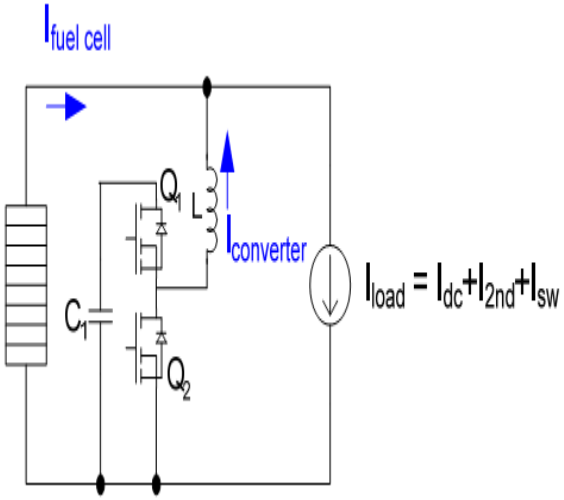

Figure 9: Proposed Converter

The pre-requisite for the operation of the proposed shunt converter is the current reference signal generation. For this, the current drawn by the power conditioner I_{load} is measured and passed through a second order low pass filter in order to get its average value. The result is then subtracted from I_{load} , thus producing a signal containing only the second harmonic ripple component and higher frequency components. This signal is then used as reference for the current controller of the proposed converter. A simplified block diagram of the controller algorithm of the converter is shown in fig. 10.

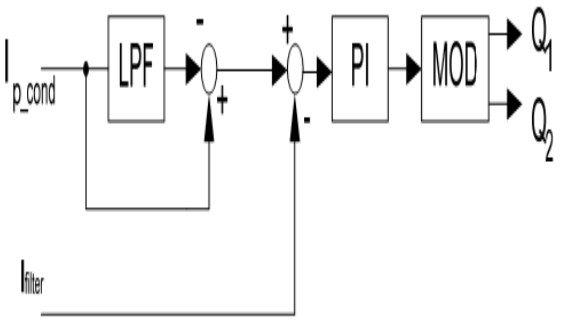

Figure 10: Current controller

VI. DESIGN OF CONVERTER

The specifications of the capacitor and inductor as well as the calculation of the voltage level required for the converter DC-link are also included in the proposed converter design as shown in fig. 9. An important factor when choosing the DC-link voltage, better known as the conversion factor (M) between the fuel cell terminal voltage and the filter capacitor voltage, is the current rating for both switches (Q1 and Q2). It has been observed from [20] that conversion ratios below M = 2 increases the current rating of the freewheeling diode in either semiconductor to up to 1.4 p.u., leading to larger semiconductors and increased conduction losses. On the other hand conversion ratios above M = 3 result in increased loses in the inductor parasitic resistance, also reducing converter efficiency. Thus it becomes convenient to choose a conversion ratio ranging between M = 2 – 3. The inductor L in the converter is designed in order to have a reduced ripple in the current supplied to the system. The current in the inductor depends on the voltage difference applied across its terminals, and since the voltage generated by the converter is Pulse Width Modulated in nature; it will consist of a second harmonic and a switching component. The inductance selection is made in order to filter out the switching component from the supplied current. Hence, the required inductance is given algebraically as:

$$L = \frac{MV_{FC}}{\Delta i \cdot I_{2nd} f_s}$$

where Δi is the maximum current ripple allowed in the inductor, I_{2nd} the magnitude of second harmonic current to be supplied, f_s the switching frequency of the converter and V_f is the no load voltage of the fuel cell. In order to specify the capacitor for the proposed converter, we consider the magnitude of the second harmonic current circulating through it and the maximum allowable DC-link voltage ripple. So, the capacitor value is calculated by:

$$C = \frac{I_{2nd}}{\omega_{2nd} \cdot \Delta_V MV_{FC}}$$

Where ω_{2nd} is the angular frequency for the second harmonic, and Δ_V is the maximum DC-link voltage ripple allowed. We now consider an example system consisting of a 48 [V] / 1000 [W] fuel cell system supplying power to a 220 [V] / 50 [Hz] single phase load through a power conditioner. From the equation of I_{d2} and assuming that the inverter operates with a 400 [V] DC-link we get the second harmonic current at the inverter input terminals to be equal to 1.78 [A]. This current is amplified by the DC-DC converter to 10.6 [A] when it is reflected at the input of the power conditioner. We choose a conversion ratio of M = 2 as discussed above which results in a filter DC-link of 96 [V]. Defining a current ripple of 20 %, a voltage ripple of 3 % and a switching frequency of 50 [kHz] one obtains that the required inductor and capacitor are L = 847 [H] and C = 4.88 [mF] respectively.

VII. SIMULATION RESULTS

To verify innovative converter operation, simulations were carried out on PSim. For this a 48V/1 kW fuel cell stack was modeled (fig. 5). This fuel cell has an internal impedance with following parameters: Voc=48 [V], R_p=1 200 [mΩ], C_1= 20 [mF], R_m= 10 [m Ω], R_{p2}= 50 [mΩ] and C_2=2[mF], corresponding to a practical fuel cell. The power conditioner unit is used to interface the fuel cell stack and the load is constructed using a push-pull DC-DC converter and single phase inverter.

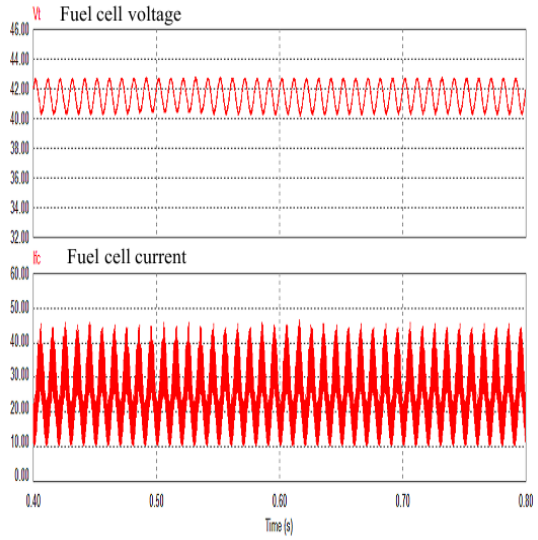

Fig. 11: System nominal operation with fuel cell voltages and currents

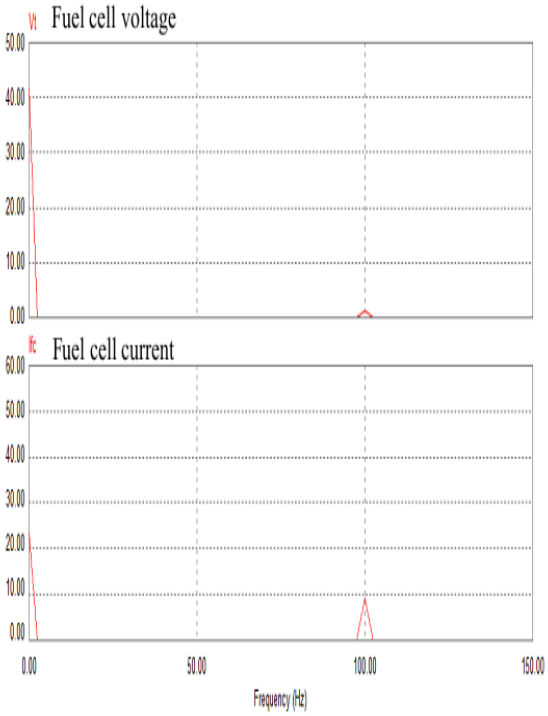

Fig. 12: Normal system operation with the spectrum of fuel cell current & voltage

The design of the push-pull converter is done for the nominal power of the stack, i.e. 1 kW, f_s being 50 kHz and a voltage gain of 10 p.u; producing a 400V DC-link. At the other side, the inverter stage was actuated with a single phase inverter switching at 10 kHz and modulated to produce 220V/ 50Hz at its output. The proposed filter was implemented using the parameters calculated in the previous section and the interaction with the system verified. Normal operation of the system is shown in fig. 11 and 12 where the fuel cell stack voltage and current are shown. From the fig. 12, we find that a significant second harmonic component exists in the frequency spectrum of the fuel cell voltage and current. In fact, the magnitude of the second harmonic current drawn from the fuel cell stack is about 40% of the DC current component which is very high in magnitude. Also, this second harmonic current when flowing through the stack produces a second harmonic voltage ripple in its voltage having a value of 2.7%.

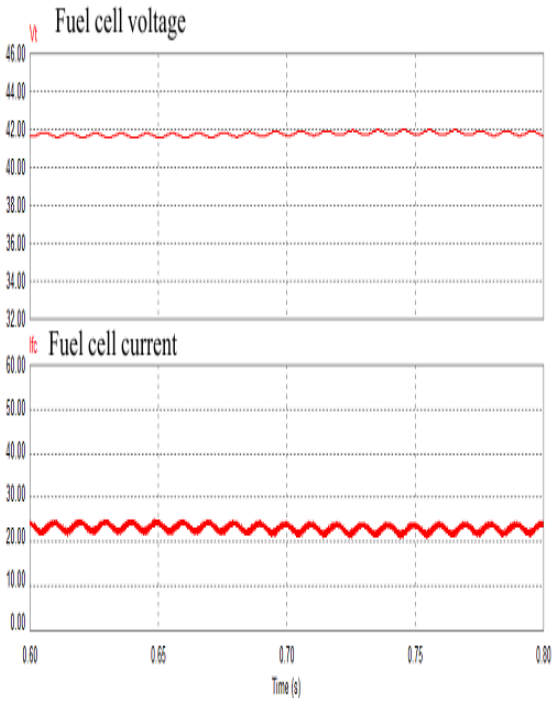

Fig. 13: System nominal operation with fuel cell voltages and currents

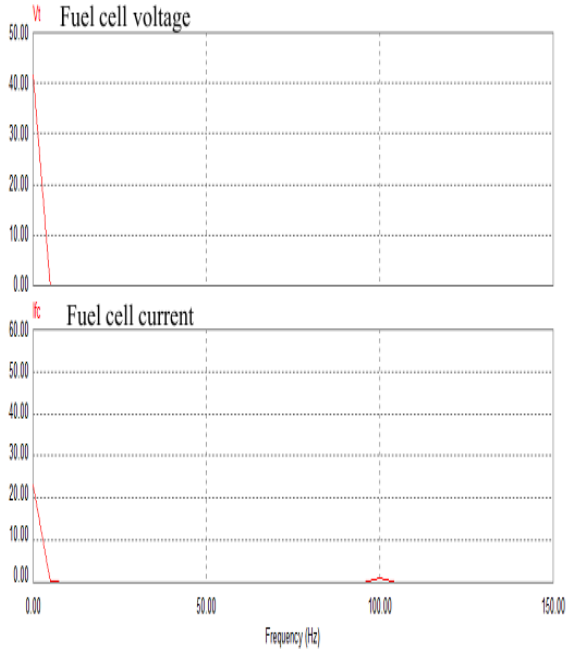

Fig. 14: Normal system operation with the spectrum of fuel cell current & voltage

After the connection of the proposed converter with the system is achieved, the simulation is repeated. Figs. 13 and 14 shows the results obtained. As can be seen from the fig. 14, the second harmonic current drawn from the fuel cell stack has been reduced drastically to 4.5% of the DC component. That is, the use of the innovative converter has reduced the presence of second harmonic current ripple by 35% when compared to normal operation. And hence, a reduction of 15% in the internal losses associated to the second harmonic current ripple is achieved. In addition it is also possible to see that there is a reduced voltage ripple in the stack terminals caused by the second harmonic current flow.

VIII. CONCLUSIONS

An active power filter has been presented in this paper as a means of reducing the low frequency current ripple. The normal operation of the power conditioner used to supply AC loads produces low frequency current components, particularly a large second harmonic current. Moreover with the help of the equivalent circuit of the fuel cell, it was deduced that this second harmonic current has the negative side effect in the fuel cell stack in the form of reduced power availability and increased internal losses. To avoid this problem an auxiliary power converter was proposed. This converter operates as a shunt active filter bringing down the magnitude of the second harmonic ripple current circulating through the stack, thus reducing the unwanted side effects of the power conditioner. The operation of the proposed converter was validated through computer simulations, and it was shown that a reduction of 37% in the second harmonic current component is possible. This in turn results in a reduction of 15% in the additional internal losses produced by the low frequency current circulation through the stack.

IX. REFERENCES

[1] S. Sumiyoshi, H. Omuri, and Y. Nishida, “Power conditioner consisting of utility interactive inverter and soft-switching DC–DC converter for fuel-cell cogeneration system,” in Proc. IEEE PCC 2007, Nagoya, Japan, pp. 455–462.

[2] R. Nojima, I. Takano, and Y. Sawada, “Transient performance o f a new-type hybrid electric power distributed system with fuel cell and SMES,” in Proc. IEEE IECON 2001, pp. 1303–1308.

[3] H. Cha, J. Choi, and B. Han, “A new three-phase interleaved isolated boost converter with active clamp for fuel cells,” in Proc. IEEE PESC 2008, pp. 1271–1276.

[4] L. Danwei and L. Hui, “A three-port three-phase DC–DC converter for hybrid low voltage fuel cell and ultracapacitor,” in Proc. I EEE IECON 2006, pp. 2258–2563.

[5] P. T. Krein and R. Balog, “Low cost inverter suitable for medium-power fuel cell sources,”in Proc. IEEE PESC 2002, pp. 321–326.

[6] B. Bouneb, D. M. Grant, A. Cruden, and J. R. McDonald, "Grid connected inverter suitable for economic residential fuel cell operation," in Proc. IEEE EPE 2005, p.10.

[7] S. Jung, Y. Bae, S. Choi, and H. Kim, "A low cost utility interactive inverter for residential fuel cell generation," IEEE Trans. Power Electron. , vol. 22, no. 6, pp. 2293–2298, Nov. 2007.

[8] J.-M. Kwon and B.-H.Kwon, "High step-up active-clamp converter with input-current doubler and output-voltage doubler for fuel cell power systems," IEEE Trans. Power Electron. , vol. 24, no. 1, pp. 108–115, Jan. 2009.

[9] D. Polenov, H. Mehlich, and J. Lutz, "Requirements f or MOSFETs in fuel cell power conditioning applications," in Proc. I EEE EPE-PEMC 2006, pp. 1974–1979.

[10] G. Fontes, C. Turpin, S. Astier, and T. A. Meynard, "Interactions between fuel cells and power converters: Influence of current harmonics on a fuel cell stack," IEEE Trans. Power Electron. , vol. 22, no. 2, pp. 670–678, Mar. 2007.

[11] M. Tavakoli Bina, Ashoka K. S. Bhat, Averaging Technique for the Modeling of STATCOM and Active Filters, IEEE Trans. Power Electron., vol. 23, No. 2, pp. 723-734, 2008

[12] C. Liu and J.-S. Lai, "Low frequency current ripple reduction technique with active control in a fuel cell power system with inverter load," IEEE Trans. Power Electronics, vol. 22, no. 4, pp. 1429–1436, Jul. 2007.

[13] S. K. Mazumder, R. K. Burra, and K. Acharya, "A ripple-mitigating and energy-efficient fuel cell power-conditioning system," IEEE Trans. Power Electronics , vol. 22, no. 4, pp. 1437–1452, Jul. 2007.

[14] F. Perfumo, A. Tenconi, M. Cerchio, R. Bojoi, and G. Gianolio, "Fuel cell for electric power generation: Peculiarities and dedicated solutions for power electronic conditioning systems," EPE J., vol 16, pp. 44–50, Feb. 2006.

[15] M. Pereira, G. Wild, H. Huang, and K. Sadek, "Active filters in HVDC systems: Actual concepts and application experience," in Proc. Int. Conf Power Syst. Technol. 2002. (PowerCon), pp. 989–993.

[16] M. Saito and N. Matsui, "Modeling and control strategy for a single-phase PWM rectifier using a single-phase instantaneous active/reactive power theory," in Proc. I EEE INTELEC 2003, pp. 573–578.

[17] X. Ma, B. Wang, F. Zhao, G. Qu, D. Gao, and Z Zhou, "A high power low ripple high dynamic performance DC power supply based on thyristor Converter and active filter," in Proc. IEEE IECON 2002, pp. 1238–1242.

[18] L.A. Moran, J.W. Dixon, R. R. Wallace, "A Three-phase Active Power Filter Operating with Fixed Switching Frequency for Reactive Power and Current Harmonic Compensation," IEEE Trans. On Ind. Elec., vol. 42, no. 4, pp. 402-408, August 1995.

[19] L. Palma, L.; M. Harfman Todorovic; Enjeti, P "Design Considerations for a Fuel Cell Powered DC-DC Converter for Portable Applications"; Applied Power Electronics Conference, APEC 2006, March 19–23, 2006, Dallas Texas.

[20] Kim, S.; Enjeti, P; "Control of Multiple Single-Phase PFC Modules with a Single Low-Cost DSP"; IEEE Transactions on Industry Applications, Vol. 39, No. 5, September/October 2003.